Calibration of a pyroelectric detector at 10.6 μm with the National Institute of Standards and Technology high-accuracy cryogenic radiometer

T. R. Gentile, J. M. Houston, G. Eppeldauer, A. L. Migdall, and C. L. Cromer

The National Institute of Standards and Technology (NIST) is establishing an infrared detector calibration facility to improve radiometric standards at infrared wavelengths. The absolute response of the cryogenic bolometer that serves as the transfer standard for this facility is being linked to the NIST high-accuracy cryogenic radiometer (HACR) at a few laser wavelengths. At the 10.6-μm CO_2 laser line, this link is being established through a pyroelectric detector that has been calibrated against the HACR. We describe the apparatus, methods, and uncertainties for the calibration of this pyroelectric detector.

1. Introduction

To meet the growing need for calibrated detectors at infrared wavelengths, the National Institute of Standards and Technology (NIST) is establishing an infrared detector calibration facility.[1] The goal of this facility is to provide absolute responsivity calibrations of detectors in the 2–20 μm spectral region with a relative expanded uncertainty of ~4% (2 sigma). To serve as a transfer standard detector, a cryogenic bolometer has been constructed.[2,3,4] The calibration of this bolometer is being linked to the NIST high-accuracy cryogenic radiometer (HACR)[5] at a few laser wavelengths. At the 10.6-μm CO_2 laser line, the link to the HACR is being established through a calibrated pyroelectric detector. In this paper we describe the apparatus, methods, and uncertainties for a calibration of the pyroelectric detector against the HACR. The transfer of the calibration from the pyroelectric detector to the bolometer will be the subject of a separate paper.

The HACR is a cryogenic electrical substitution radiometer that serves as a primary standard for optical power measurements and has been used to measure radiant power at visible wavelengths with a relative standard uncertainty of 0.021%. The HACR is best suited for measurements at an optical power level of between 0.1 and 1 mW, but the response of the bolometer becomes nonlinear at power levels above a few microwatts. Hence an indirect calibration is performed. First a pyroelectric detector is calibrated against the HACR, and then the cryogenic bolometer is calibrated against the pyroelectric detector. This approach is also convenient because the pyroelectric detector is compact, easily portable, relatively simple to use, and operates at room temperature. Its dynamic range is suitable for bridging the range between several microwatts and 1 mW, although a somewhat lower noise floor would be desirable. The main disadvantage of the pyroelectric detector is the spatial nonuniformity in its response. Although a thermopile detector was tested as an alternative transfer detector, we chose the pyroelectric detector because of reduced susceptibility to noise due to thermal drift.

We describe the apparatus and methods of the calibration in Section 2 and the measurement results and uncertainties in Section 3.

2. Apparatus

A. High-Accuracy Cryogenic Radiometer

As the HACR has been described in detail elsewhere,[5] here we provide only a brief overview of the instrument. A diagram is shown in Fig. 1. The HACR is an electrical substitution radiometer operated just above the boiling point of liquid helium. An electrical substitution radiometer links a measurement of optical power to the watt by comparing the temper-

The authors are with the National Institute of Standards and Technology, Gaithersburg, Maryland 20899.

Received 3 September 1996; revised manuscript received 2 January 1997.

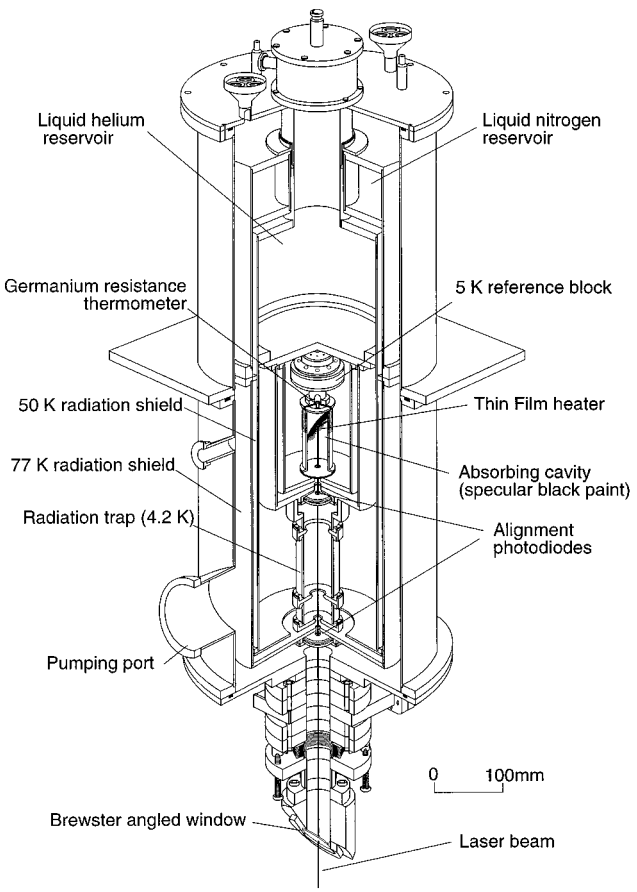

Fig. 1. Diagram of the NIST high-accuracy cryogenic radiometer.

ature rise induced in an absorbing mass by incident optical radiation to that obtained by electrical heating. The absorbing mass is a cavity designed for nearly complete absorption of laser radiation. Operation at cryogenic temperatures allows a large, highly absorptive cavity to be used without significantly increasing the time constant, and the radiative coupling of the cavity to its surroundings is reduced. These features improve the equivalence of optical and electrical heating. However, cryogenic operation also requires a vacuum Dewar, necessitating a window between the cavity and the laboratory. To reduce the reflection loss, this window is oriented at the Brewster angle, and appropriately polarized light is used. To facilitate alignment of the laser light into the cavity and to measure the amount of laser light scattered out of the beam, two sets of four annular quadrant silicon photodiodes, each 50 mm in diameter with a 9-mm-diameter central aperture to pass the beam, are located along the optical path within the HACR. (Although these detectors were not directly usable with the infrared beam, they were used with a visible alignment beam that was spatially overlapped with the infrared beam.) The apertures in the quadrant photodiodes are the limiting apertures in the HACR.

B. Laser System

The laser system is shown in Fig. 2. As with the apparatus previously described for visible wavelengths,[5] the primary goal is to generate a geometrically well-defined beam with stable power. The power was stabilized using an acousto-optic laser stabilizer[6] with an external feedback detector. A well-defined beam spatial profile was obtained using a spatial filter with an overfilled pinhole. Because the output power of the CO_2 laser is 4 orders of magnitude higher than the level that can be used with the HACR, it was also necessary to attenuate the laser. While this could be accomplished with either attenuating filters or nearly crossed polarizers, both methods have disadvantages. A filter's attenuation could be affected by temperature rise induced by high

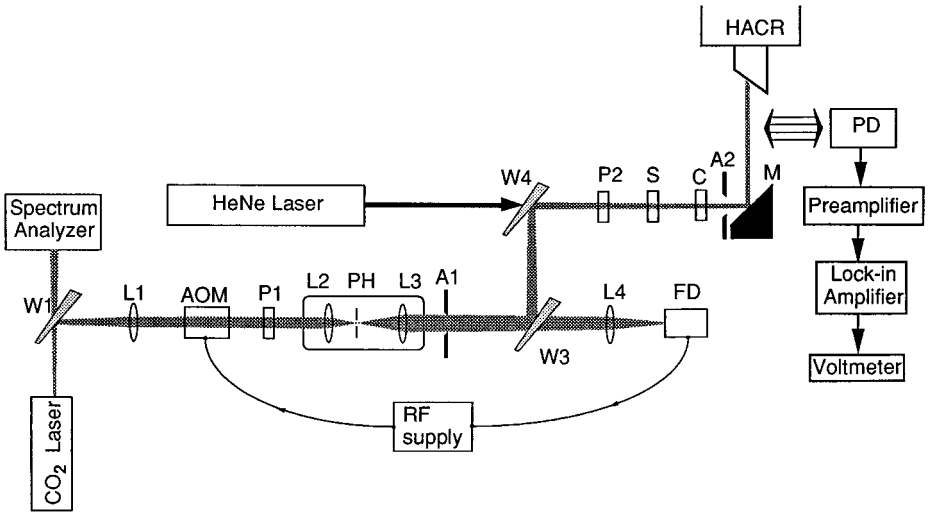

Fig. 2. Diagram of the laser system. W1, W3, W4, ZnSe-wedged windows (there is an additional wedged window W2 located just before L2 that is not shown); L1, L2, L3, L4, ZnSe lenses; AOM, acousto-optic modulator; P1, P2, polarizers; PH, pinhole; A1, A2, apertures; FD, HgCdTe feedback detector; S, shutter; C, chopper; M, steering mirror; PD, pyroelectric detector. The reflection from the steering mirror is out of the plane of the diagram.

power levels, while crossed polarizers could degrade the polarization purity of the beam. Because of these drawbacks, most of the attenuation was accomplished by reflecting the beam from ZnSe-wedged windows instead of steering mirrors. For each window, only one of the reflected beams was used, while the other reflected beam was blocked. An attenuation factor of ~300 was obtained from the four wedged windows in the system. This approach also provided monitor beams and a method for overlapping the alignment He–Ne beam with the CO_2 beam, as described below.

The source was a 5-W, air-cooled, grating-tuned, vertically polarized CO_2 laser operated with a frequency stabilizer. The laser was operated on the $P(20)$ line [wavelength equals 10.5910 μm (Ref. 7)], with a TEM_{00} transverse mode. After exiting the laser, the diverging beam was reflected by a wedged window (W1), collimated by a ZnSe lens (L1), and passed through an acousto-optic modulator (AOM) that is part of a power stabilizer. (The beam transmitted through W1 was used to monitor the laser's output power or to determine its wavelength using a CO_2 spectrum analyzer.) When rf power is applied to the AOM, a fraction of the laser light is deflected into a secondary beam, thereby providing control of the power in the primary beam. Farther down the beam path, a HgCdTe feedback detector (FD) sampled the beam and provided the input to the stabilizer's feedback circuit. This system maintained the power of the laser beam to within 0.1% over the course of an hour. The feedback detector was located as far downstream in the beam path as possible within the constraint of this detector's sensitivity.

After the AOM, the beam passed through a polarizer (stack of six ZnSe plates, P1) and was reflected from another wedged window (referred to as W2, but not shown). For most of the measurements this polarizer simply improved the vertical polarization of the beam, but it was also used in conjunction with a wire grid polarizer located farther downstream (P2) for relatively minor attenuation of the beam (less than a factor of 3). The beam was attenuated by rotating P1, while the polarizer P2 reestablished the vertical polarization required to minimize the reflectance from the Brewster window. The polarization of the beam incident upon P2 was nearly vertical because vertically polarized light is preferentially reflected from the wedged windows. When additional attenuation was required, a thin 12% transmitting filter (25-nm-thick layer of NiCr deposited on 100-nm-thick substrate) was placed just before P2. Using a thin filter avoided possible interference effects and deflection of the beam.

A well-defined beam spatial profile was obtained by using a spatial filter with an overfilled pinhole. The laser light was focused with a 8-cm focal length ZnSe lens (L2) onto a 250-μm-diameter pinhole (PH). This beam overfilled the aperture, creating an Airy diffraction pattern. (The amount of overfilling was also used to attenuate the beam by a factor of between 2.5 and 7.) The diameter of an iris (A1) was adjusted to allow only the 13-mm-diameter central spot of the diffraction pattern to pass through. The diameter of the aperture corresponded to the location of the first minimum of the diffraction pattern, thus defining the beam diameter with minimal scattering from the aperture. A 12.5-cm focal length ZnSe lens (L3) produced a long beam waist between the pyroelectric detector (PD) and the limiting apertures inside the HACR dewar. At the waist, 85% of the power fell within a 3-mm beam diameter and 99% within a 5 mm diameter. The beam was then reflected from another wedged window (W3), while the transmitted beam was focused by a ZnSe lens (L4) onto the feedback detector. Finally, the beam was reflected from the last wedged window (W4), where it was spatially overlapped with a visible alignment beam. The alignment beam was provided by a He–Ne laser and prepared with a similar optical system (not shown). The total attenuation of the CO_2 laser beam along the optical path to the HACR was a factor of 3000 or more, reducing the 3-W output power of the laser down to 1 mW or less.

The polarizer P2 was adjusted to minimize the reflection from the ZnSe Brewster window on the HACR, and a mirror (M) reflected the laser light into the HACR. (This reflection is out of the plane of Fig. 2.) Whereas the final steering mirror could affect the polarization of the beam if the direction of the polarization were at an arbitrary angle to the plane of incidence, this effect was negligible in this system because the light was polarized parallel to the plane of incidence of the mirror. A computer-controlled shutter (S) was used to block the laser during electrical heating of the cavity and to measure the background signal from the pyroelectric detector. A chopper (C), which is required for use with the pyroelectric detector, was located after the shutter and operated at a chopping frequency of 40.0 Hz. In addition, an 8-mm-diameter aperture (A2) located just before the final steering mirror was used to block residual scattered laser light.

The infrared beam was aligned into the HACR by being spatially overlapped with the He–Ne laser. Although the alignment of a visible beam into the HACR is usually optimized by minimizing the scattered light signal from the quadrant photodiodes, the sensitivity of this method was limited by the high level of scatter from the ZnSe Brewster window at 633 nm. Instead, the diameter of the He–Ne beam was made to be larger than the infrared beam, in fact, nearly as large as the apertures in the annular quadrant photodiodes. This approach provided a sensitive method to align the He–Ne beam into the HACR. After this alignment procedure, the He–Ne beam was blocked. The difference between the displacement of the He–Ne and CO_2 beams due to the ZnSe Brewster window is only 0.15 mm. The alignment was tested by establishing that the temperature rise of the cavity due to the infrared beam was a maximum and not unduly sensitive to small changes in the alignment of the final steering mirror. As described below, small changes were also made in the alignment to test for

change in the measured responsivities of the pyroelectric detectors.

C. Pyroelectric Detectors

Lithium tantalate detectors, coated with black paint to absorb infrared light, were calibrated against the HACR. A pyroelectric material has a permanent electric dipole moment. A change in the temperature of the material changes the magnitude of this moment, requiring a flow of charge. If a chopped source of optical power is absorbed by a pyroelectric material, the resulting time variation in its temperature will produce a measurable ac current. This current can be detected by use of a lock-in amplifier, with the chopping frequency used as the reference.[8]

Two 1 cm × 1 cm pyroelectric detectors,[9] here referred to as PD1 and PD2, were calibrated against the HACR. These particular pyroelectric detectors were chosen because of their large area. Unfortunately, as discussed below, the black paint coating supplied with the detector proved to have lower than desired absorption in the infrared. For the most part, we will describe and show data only for PD2, which is being used to calibrate the bolometer. The results for PD1 are comparable, but because of accidental damage that occurred during the course of this work, its spatial uniformity was degraded. We also calibrated a third pyroelectric detector that is part of a commercial electrical substitution pyroelectric radiometer (ECPR). This detector was calibrated with and without the electrically calibrating circuitry operational.

PD1 and PD2 were each mounted in a small aluminum box with a 13-mm-diameter entrance aperture. The boxes were mounted on a computer-controlled, motor-driven carousel, which positioned each detector in the infrared beam. Atmospheric absorption between the pyroelectric detector and the HACR is $<0.01\%$ (Ref. 10) and was neglected. To minimize the uncertainty due to the spatial response nonuniformity of the detector, we used an algorithm for reproducibly positioning the detector in the infrared beam: For each of the two axes transverse to the beam, the detector was positioned midway between the two locations at which the detector response was 50% of its maximum value.

The spatial nonuniformity observed in the response of PD2 is shown in Fig. 3. We obtained these data by scanning the detector over a 6 mm × 6 mm region in 0.5-mm steps, using the same size beam as was used for the calibrations. For the region within 0.5 mm (2 mm) of the center, the maximum variation in the detector response is $\pm 0.8\%$ ($\pm 2.6\%$) and is primarily along one direction. This rather substantial nonuniformity is likely to vary from detector to detector and could be improved with a better absorbing coating. We estimate the reflectance of the pyroelectric detector to be at least 25% at 10.6 μm, based on comparing the responsivity at 10.6 μm to that measured at 633 nm with a calibrated visible detector.[11] (The value of 25% assumes that the reflectance is close to zero at 633 nm.) Using a half-wave plate to rotate the polarization of the infrared beam, we found the polarization dependence of the detector's responsivity to be $<0.05\%$.

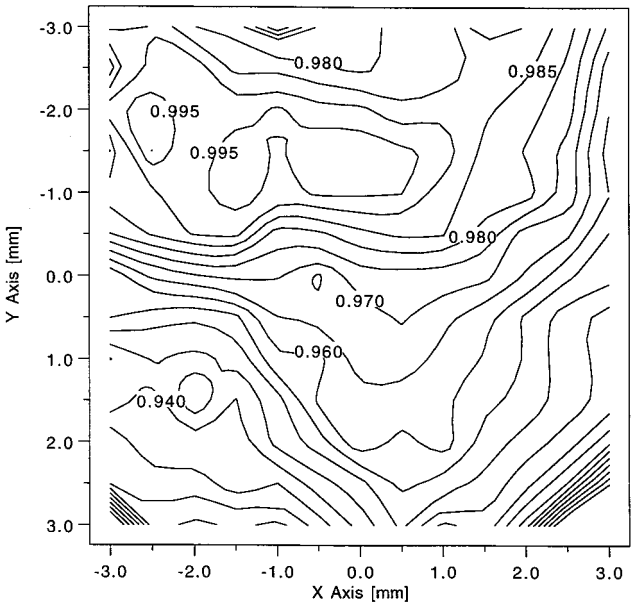

Fig. 3. Contour plot illustrating the spatial uniformity of the responsivity of pyroelectric detector PD2. These data were obtained by scanning of the 3-mm-diameter beam (85% of power) in 0.5-mm steps.

The temperature dependence of the responsivity for lithium tantalate is weak. The responsivity is proportional to the ratio of the pyroelectric coefficient to the specific heat. The temperature dependence of this ratio was measured by Glass and Lines[12]; from their data one can estimate the expected temperature dependence of the responsivity to be $0.1\%\ \mathrm{K}^{-1}$ at room temperature. Using a temperature-controlled box, we measured $0.16\%\ \mathrm{K}^{-1}$, roughly consistent with the predicted result.

This work was carried out over a period of a few months, during which time we saw no evidence for any long-term change in the calibration of the pyroelectric detectors. However, the stability of these detectors over a period of years remains to be established.

D. Measurement Instrumentation

The output signal from each detector was sent to a transimpedance amplifier with a gain of 10^8 V/A, and then to a lock-in amplifier that was sensitive to only the fundamental Fourier component of the waveform at the chopping frequency. The in-phase output of the lock-in amplifier was read by a digital voltmeter. The phase was set manually to minimize the out-of-phase signal. The component of relative standard uncertainty in the responsivity S due to the uncertainty in setting the phase was 0.02%.

The system, consisting of the pyroelectric detector and preamplifier, was calibrated as a unit. The responsivity was defined to be the amplitude of the ac voltage output from the preamplifier, assuming a per-

fectly square optical waveform, for a given dc optical power that would be incident on the detector if the chopper were removed. The responsivity is given by

$$S = VC_d/GC_sP_L, \quad (1)$$

where V is the in-phase output of the lock-in amplifier in millivolts, G is a correction factor for the absolute response of the lock-in, P_L is the infrared power in mW as determined by the HACR, C_d is the chopper duty cycle, and C_s is a small correction factor associated with the deviation of the optical waveform from a perfect square wave (described below). Because the HACR has a 4-min time constant, P_L is the average power in the chopped beam.

We determined the chopper duty cycle by measuring the ratio of the infrared power with the chopper turned on to that obtained with the chopper off. Because the pyroelectric detector responds only to chopped radiation, it was necessary to install a second chopper in the beam path. Operating the second chopper at a much higher frequency (400 Hz) allowed lock-in detection at the second chopper's frequency without interference from the primary chopper. The duty cycle was independently determined with the HACR and also with a He–Ne laser and a visible detector. We obtained $C_d = 0.4964$ with a standard uncertainty of 0.001.

The measured responsivity of the entire system was found to change by 0.25% Hz^{-1} at the 40.0-Hz chopping frequency. This dependence was almost entirely due to the preamplifier's 3-dB point at 110 Hz. (This preamplifier, originally designed for dc applications, was used simply because it could be immediately dedicated to these measurements and may be replaced in the future.) For a standard uncertainty of ± 0.1 Hz in the chopper frequency, the relative standard uncertainty in the responsivity is only 0.025%.

The magnitude of the fundamental component in the output from the pyroelectric detector depends on the shape of the optical waveform, which is primarily determined by the beam size and the chopper blade geometry. The two-blade chopper has an inner diameter of 5 cm and an outer diameter of 11 cm, which yields a mean chopper opening width of 6.3 cm. Thus, for a beam diameter of 5 mm at the chopper, the output of the preamplifier should exhibit a rise time of only 8% of the half-period, which is due only to the chopper. (The observed rise time was roughly twice this value, owing to the limited frequency response of the preamplifier.) We have corrected the measured responsivities to the ideal conditions of a perfectly square optical waveform, which would only be obtained with an infinitely narrow beam. To determine this correction, labeled C_s in Eq. (1), we measured the effect on the responsivity of changing the beam diameter at the chopper from 6 mm to under 1 mm and found $C_s = 0.9980$ with a standard uncertainty of 0.0005. (Because this correction is independent of the detector used, these measurements were performed more easily at a visible wavelength.) Because this correction is small, the calibration is quite insensitive to the beam size and spatial profile.

To determine the correction G for the absolute response of the lock-in amplifier, we used a square wave with a known amplitude. We obtained this square wave by illuminating a silicon photodiode with a chopped He–Ne laser beam. The detector's output was sent to a fast transimpedance amplifier. We determined the amplitude of the square wave by turning off the chopper and measuring the dc voltage from this amplifier with a high accuracy digital voltmeter. (The uncertainty in the measurement of dc voltage is negligible.) This measurement was performed with the lock-in amplifier on the 500-mV range. A range-to-range correction factor was determined for the 10-mV range, which was used for most of the pyroelectric detector measurements. The total correction factor for the 10-mV range was $G = 0.9023$ with a standard uncertainty of 0.002. Note that a 1-V amplitude square wave, sent into an ideal sine-wave lock-in amplifier, produces an output of 0.9003 ($=4/\pi\sqrt{2}$) V. The value of G for each of the other ranges that were used with the pyroelectric detectors were also measured; these correction factors were typically within 1% of 0.9003 and were measured with a relative standard uncertainty of 0.1%.

E. Measurement Sequence

The details of the automated sequence for HACR measurements are described in Ref. 5. Briefly, the sequence consists of one optical measurement cycle, in which the temperature rise of the cavity due to the laser light is determined, followed by electrical heating, in which the quantity of electrical power required to reproduce this temperature is determined. The entire sequence takes ~45 min. The response of the pyroelectric detectors was measured during the electrical heating cycle.

3. Measurement Results and Uncertainties

A. Measurement Results

The results of several responsivity measurements of PD2 are summarized in Table 1 and shown in Fig. 4. Each data point is the mean responsivity for a given session of data acquisition, in which typically 15–20 measurements were obtained. We calibrated the detector over an infrared power range from 0.011 to 0.35 mW, with no other deliberate change in conditions. (These data are the first seven entries in Table 1 and are shown by filled circles in Fig. 4.) As described below, this series of measurements allowed us to establish an uncertainty due to background effects. For the remaining data points, small changes were made in the measurement conditions to test the sensitivity to certain systematic effects that are discussed below. (These data are the last four values in Table 1 and are shown by open squares in Fig. 4.)

In Fig. 4, the uncertainty bar shown on each data point corresponds to the relative standard deviation

Table 1. Measured Values of the Responsivity S of the Pyroelectric Detector PD2 for a Range of Infrared Power Levels and Other Variations in the Conditions of the Calibration[a]

P_L (mW)	S (mV/mW)	σ_m/S (%)	$(S - S_a)/S_a$ (%)
0.3397	6.880	0.03	−0.17
0.3392	6.893	0.04	0.03
0.3203	6.897	0.03	0.09
0.2599	6.894	0.02	0.04
0.07379	6.880	0.11	−0.16
0.03079	6.873	0.21	−0.26
0.01375	6.815	0.41	−1.11
1.051	6.904	0.10	0.18
0.3395	6.888	0.02	−0.04
0.3421	6.924	0.01	0.48
0.3368	6.849	0.04	−0.61

[a]The mean responsivities of the relative standard deviation of the mean, σ_m/S, are listed for each session of data acquisition. The percentage deviation of each responsivity from the average responsivity (S_a = 6.89 mV/mW) is also listed; the average is based on the data obtained at power levels above 0.2 mW.

of the mean in the measurements of S for the given session. (For the results at 1.05 mW and below 0.2 mW, which were not obtained on the 10-mV lock-in range, an additional contribution of 0.1% has been added in quadrature to yield the total uncertainty bar.) The increased standard deviation at low values of P_L is due to comparable contributions from the noise floors of the HACR[5] and the pyroelectric detector. The slight decrease in responsivity at the lowest power levels could indicate a systematic effect associated with background subtraction. This decrease was seen for both pyroelectric detectors but not for the ECPR, which suggests a possible systematic error in the calibration of the pyroelectrics. However, fitting the data to a form that models such a background error[5] yielded a relative standard uncertainty component of 0.05% at our typical calibration power of 0.35 mW.

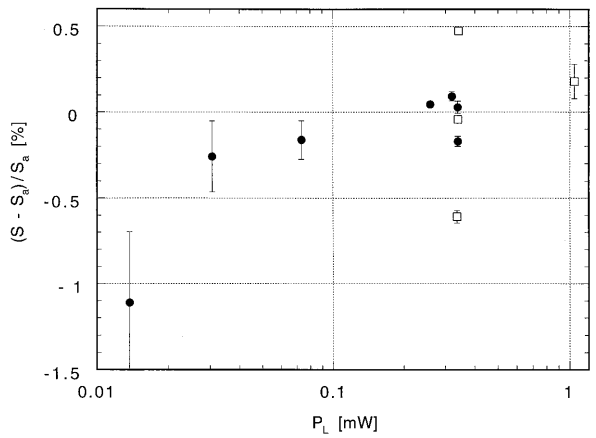

Fig. 4. Percentage deviation of each responsivity S listed in Table 1 from the average responsivity S_a; the average is based on the data obtained at power levels above 0.2 mW. The data shown by filled circles were obtained with no deliberate change in conditions to test for linearity of the detector and background effects. The data shown by open squares include changes in the conditions of the measurements that are described in the text.

We now restrict the discussion to the data obtained at power levels of 0.2 mW or above. For a typical session of data acquisition, the relative standard deviation in repeated measurements for either V or P_L was typically 0.15%. The primary source of this variation was drift in the power of the infrared beam. For S the relative standard deviation was only 0.1% or less because slow drift in the infrared power does not affect the measurement of S.

The data shown by open squares were obtained with small changes to the calibration conditions. These changes included removing the detector from the carousel, repeating the alignment algorithm, and small variations in the alignment of the laser beam into the HACR. The goal of these changes was to establish the reproducibility of the calibration, given the known spatial nonuniformity of the detector and the difficulty in aligning the infrared beam into the HACR. (For our work here we are primarily interested in our ability to reproducibly calibrate the detector using our alignment algorithm. The related, but separate, issue of the transfer of this calibration to the cryogenic bolometer will be discussed in another paper.)

We determined the average responsivity (S_a = 6.89 mV/mW) by averaging the data obtained at power levels above 0.2 mW. The relative standard deviation of this data set is 0.31%, which is substantially larger than the relative standard deviation of the mean for any given session of data acquisition. Hence the reproducibility of the calibration was affected by both unintentional and imposed changes in calibration conditions. The small relative standard uncertainty of ±0.05% that is due to the typical variations of ±0.3 K in the ambient laboratory temperature can account for only a small portion of the observed 0.31% relative standard deviation. We believe the most likely cause is the known spatial nonuniformity of the detector. From Fig. 3 we see that a change of ±0.2 mm in the location of the detector or the beam can result in a ±0.3% change in the measured responsivity. We believe that spatial uniformity could explain most of the observed variation in the measurements of S. We assign a type A relative standard uncertainty[13] of 0.31% to the reproducibility of the calibration, which includes effects of spatial nonuniformity and beam alignment.

As a final test of the quality of the alignment into the HACR, we shifted the location of the focus farther along the beam path so that it was between the two limiting apertures in the HACR. If the beam had been slightly obstructed by these apertures, shifting the focus would cause the measured responsivity to decrease. We observed a decrease of 1.0% in the measured responsivity for detector PD2, whereas the responsivity of PD1 was nearly unchanged. This suggests that the effect was not due to alignment into the HACR but some other effect that was different for the two detectors. Changing the location of the focus did require realigning the detectors and also in-

Table 2. Components of the Combined Relative Standard Uncertainty of 0.48% in the Calibration of the Pyroelectric Detector Transfer Standard Against the HACR at an Optical Power Level of 0.35 mW[a]

Uncertainty Component	Type	Value of Correction	Component of Uncertainty (%)
Reproducibility	A		0.31
Background	A		0.05
G	B	0.9023	0.20
C_d	B	0.4964	0.20
C_s	A	0.9980	0.05
Chopper frequency and lock-in phase	B		0.03
Combined standard uncertainty in P_L	B		0.21
Window transmittance (T)		0.9978	0.18
Scattered optical power (P_S)		0.61 μW	0.1

[a]The uncertainties are identified as type A or type B relative standard uncertainties. The measured values of corrections to the data are also listed.

creased the beam size at the detectors a small amount. These changes, in conjunction with the spatial nonuniformity of the detectors, could explain the observed 1.0% shift in the responsivity for PD2. Hence we have not increased the uncertainty in the reproducibility in the calibration because of this measurement.

B. Corrections for Window Transmittance and Scattered Laser Light

The uncertainty components in these calibrations are listed in Table 2. The method used to evaluate each uncertainty component (type A or type B) is also listed. We now discuss the combined uncertainty component in the measurement of P_L by the HACR. The infrared power P_L is given by

$$P_L = (1/T)[(NP_H/A) + P_S]. \quad (2)$$

where P_H is the electrical heater power that yields the same temperature rise of the cavity as that produced by the infrared beam, P_S is the estimated infrared power scattered out of the field of view of the cavity, A is the absorptance of the cavity, T is the transmittance of the entrance window of the HACR, and N is a factor to take into account any nonequivalence between the infrared and electrical heating. For this work, the type B uncertainty in the measurement of P_L by the HACR is dominated by the uncertainties in T and P_S, which are discussed in detail below. Other HACR uncertainties discussed in Ref. 5 are less than 0.01%, which is negligible for this work.

The transmittance of the window was measured on the optical table before and after the series of measurements with the HACR. Although this is a simple measurement in principle, care was required because of the nonuniformity of the available detectors. The transmittance was determined by measuring the signal on a pyroelectric detector with and without the window in the beam. Because the window translates the beam, the detector must also be translated so that the beam is still incident upon the same location on the detector. Any error in this relocation leads to an error in the measured transmittance. We measured a transmittance of 0.9993 ± 0.0004 before the series of HACR measurements and 0.9962 ± 0.0008 afterward, where the uncertainties quoted are the standard deviations of the mean for each group of measurements (16 measurements for the before data and 7 for the after data). These transmittance measurements were separated by 4 months, and we believe that the decrease in transmittance was due to accumulation of contaminants on the window. We used the average value of T = 0.9978 ± 0.0018 to determine P_L, where the standard uncertainty quoted is equal to the sum of half the difference between the before and after values, plus the uncertainties quoted for the before and after data, added in quadrature.

Before measuring the transmittance, the window reflectance was minimized by adjusting the polarizer P2 and the angle of incidence of the beam on the window. We minimized the reflection, rather than maximizing the transmittance, so that the procedure was the same as that performed when the window was installed in the HACR. (Because of the slow time constant of the HACR, it is difficult to maximize the transmittance by observing the temperature of the cavity.) Furthermore, we measured the reflectance to establish that the same value was obtained when the window was installed in the HACR. Using one of the pyroelectric detectors, we measured the reflectivity of the window to be 0.1% ± 0.03%.

Scattered laser light refers to light that is incident upon the detector to be calibrated but scattered out of the field of view of the absorbing cavity in the HACR. For visible wavelengths there is little scattered laser light, and it is measured by annular silicon photodiodes located along the optical path within the HACR. Because scattered infrared laser light cannot be measured by the photodiodes in the HACR, we estimated the correction for scattered laser light by simulating the usual trajectory of the beam into the HACR on the optical table: Just before the final steering mirror, the beam was deflected with a mirror. A window was placed in the beam where the HACR window would normally be located. To col-

lect only the scattered light, we used a 15-cm focal-length concave mirror with a 9-mm central aperture. This mirror was located near the position of the quadrant photodiodes in the HACR dewar, which also have 9-mm-diameter apertures. Detector PD1 was used to detect the reflected light from this mirror. We measured P_S to be 0.18% of the incident infrared power. Most of this scattered light was not due to the window. It is difficult to establish how close this measurement is to the actual value that P_S was during our calibrations. On the basis of the repeatability of the measurement and the sensitivity to changes in the beam alignment, we estimate an relative standard uncertainty component of 0.1% due to scattered light, about half the value of the correction itself.

4. Conclusion

We have calibrated a pyroelectric detector against the HACR at a wavelength of 10.6 μm with a combined relative standard uncertainty of 0.48%. This detector is being used to calibrate the transfer standard cryogenic bolometer for an infrared comparator facility. The calibration of the bolometer, which is being performed with a different laser system, will be discussed in another paper. The primary issue in the accuracy of the bolometer calibration is the spatial uniformity of the pyroelectric detector. Minimizing this uncertainty requires reproducing the alignment procedure and beam characteristics that were used for the HACR calibration. We believe that the transfer of this calibration can easily be done with a conservative relative standard uncertainty of ±2%, and with careful attention to detail, a relative standard uncertainty of ±0.6% should be achievable.

We are investigating detectors with improved spatial uniformity, which can be obtained by using gold-black coatings or a light-trapping arrangement.[14,15] Colleagues in our laboratory have produced gold-black coatings with less than 1% reflectance at the CO_2 laser wavelength. An alternative solution is to calibrate the cryogenic bolometer directly against the HACR. This approach would require improving the sensitivity of the HACR, attenuating the beam for the bolometer by a precisely known amount, further quantifying the bolometer's nonlinearity, or some combination of these changes. Finally, work is in progress at NIST to develop a large-area silicon bolometer that could have both high sensitivity and a sufficiently large dynamic range to be used easily with the HACR.

References and Notes

1. A. Migdall, G. Eppeldauer, and C. Cromer, "IR detector spectral responsivity calibration facility at NIST," in *Cryogenic Optical Systems and Instruments VI*, J. B. Heaney and L. G. Burriesci, eds., Proc. SPIE **2227,** 46–53 (1994).
2. G. Eppeldauer, A. L. Migdall, and C. L. Cromer, "Characterization of a high sensitivity composite silicon bolometer," Metrologia **30,** 317–320 (1993).
3. G. Eppeldauer, A. L. Migdall, and C. L. Cromer, "A cryogenic silicon resistance bolometer for use as an infrared transfer standard detector," in *Thermal Phenomena at Molecular and in Cryogenic Infrared Detectors*, M. Kaviany, D. A. Kaminskii, A. Majumdar, P. E. Phelan, M. M. Yovanovich, Z. M. Zhang, eds. (American Society of Mechanical Engineers, New York, 1994), Vol. 277, pp. 63–67.
4. G. Eppeldauer, A. L. Migdall, T. R. Gentile, and C. L. Cromer, "Absolute response calibration of a transfer standard cryogenic bolometer," in *Photodetectors and Power Meters II*, K. Murray and K. J. Kaufmann, eds., Proc. SPIE **2550,** 36–46 (1995).
5. T. R. Gentile, J. M. Houston, J. E. Hardis, C. L. Cromer, and A. C. Parr, "National Institute of Standards and Technology high accuracy cryogenic radiometer," Appl. Opt. **35,** 1056–1068 (1996).
6. Model LS-10.6, Cambridge Research and Instrumentation, Inc., 21 Erie Street, Cambridge, Mass. 02139. Certain trade names and company products are mentioned in the text or identified in an illustration in order to adequately specify the experimental procedure and equipment used. In no case does such identification imply recommendation or endorsement by the National Institute of Standards and Technology, nor does it imply that the products are necessarily the best available for the purpose.
7. R. J. Pressley, ed., *Handbook of Lasers With Selected Data on Optical Technology* (CRC, Cleveland, Ohio, 1971), p. 331.
8. R. W. Boyd, *Radiometry and the Detection of Optical Radiation* (Wiley, New York, 1983), pp. 219–223.
9. Servo Corporation of America, 111 New South Road, Hicksville, New York 11802-1490.
10. W. L. Wolfe and G. J. Zeissis, eds., *Infrared Handbook*, 3rd ed. (Infrared Information Analysis Center, Environmental Research Institute of Michigan, Ann Arbor, Mich., 1989), pp. 5–69.
11. T. R. Gentile, J. M. Houston, and C. L. Cromer, "Realization of a scale of absolute spectral response using the NIST high accuracy cryogenic radiometer," Appl. Opt. **35,** 4392–4403 (1996).
12. A. M. Glass and M. E. Lines, "Low-temperature behavior of spontaneous polarization in $LiNbO_3$ and $LiTaO_3$," Phys. Rev. B **13,** 180–191 (1976).
13. B. N. Taylor and C. E. Kuyatt, "Guidelines for evaluating and expressing the uncertainty of NIST measurement results," Tech. Note 1297, 2nd ed. (National Institute of Standards and Technology, Gaithersburg, Md., 1994).
14. D. J. Advena, V. T. Bly, and J. T. Cox, "Deposition and characterization of far-infrared absorbing gold black films," Appl. Opt. **32,** 1136–1144 (1993).
15. R. J. Phelan, Jr., J. Lehman, and D. R. Larson, "Electrically calibrated pyroelectric detector—refinements for improved optical power measurements," in *Photodetectors and Power Meters*, K. J. Kaufmann, ed., Proc. SPIE **2022,** 160–163 (1993).